T H E U N I V E R S I T Y O F M I C H I G A N
COLLEGE OF ENGINEERING
Department of Electrical Engineering
Space Physics Research Laboratory

Scientific Report No. 3

APPLICATION OF A QUASI-OPEN ION SOURCE FOR NEUTRAL PARTICLE DENSITY MEASUREMENTS IN THE THERMOSPHERE

Hasso B. Niemann
John R. Kreick

ORA Project 07065

under contract with:

NATIONAL AERONAUTICS AND SPACE ADMINISTRATION
GODDARD SPACE FLIGHT CENTER
CONTRACT NO. NAS 5-9113
GREENBELT, MARYLAND

administered through:

OFFICE OF RESEARCH ADMINISTRATION ANN ARBOR

August 1966

TABLE OF CONTENTS

LIST OF FIGURES

ABSTRACT

An open ion source Mass Spectrometer is used with an Omegatron Mass Spectrometer in the Thermosphere Probe Experiment to measure atmospheric gas density and composition. Expressions are given relating the ambient number density of each gas to the gas density in the ionization region and suggestions are made on how they should be applied.

Possible recombination and thermal accommodation of the gases on the probe surfaces are considered and coatings are suggested for optimal accuracy.

INTRODUCTION

In the Thermosphere Probe experiment, two mass spectrometers, a Quadrupole and an Omegatron, will be used simultaneously to measure gas density, composition, and temperature in the upper atmosphere. The Thermosphere Probe, shown in Fig. 1, is an ejectable instrument developed to carry a variety of measuring devices into the thermosphere. The Quadrupole and the Omegatron will occupy opposite ends of the cylinder; the remaining space is occupied by other experiments and auxiliary subsystems which make the probe completely self-contained.

Before launch, the Quadrupole and the Omegatron are calibrated together on an ultra-high vacuum system for the various gases which they will measure. While under this high vacuum, both instruments are sealed and inserted into the Thermosphere Probe. The seals are not broken until the Thermosphere Probe is ejected from the launch vehicle into the thermosphere. This procedure guards against contamination of the instruments and reduces the time required for the gauge volume to reach equilibrium with the atmosphere.

When the probe is ejected from the launch vehicle, it is caused to tumble so that the cylinder rotates in a plane with a constant angular frequency. Since the Quadrupole and Omegatron are located on the ends of the cylinder, their orientations with respect to the velocity vector of the center of mass of the probe vary periodically with time. The initial calibration of the instruments alone is not sufficient to handle this situation, since in the calibration particles possess only random thermal velocity with respect to the instruments. The Omegatron mass spectrometer is coupled to the atmosphere through a knife edge orifice permitting the use of the well known "F(s)" relationship (Ref. 1) to treat the moving instrument. The ionizing source of the Quadrupole Spectrometer is immersed in the atmosphere. In this paper expressions are derived which relate this case of the moving instrument (or moving gas) to that of the stationary instrument.

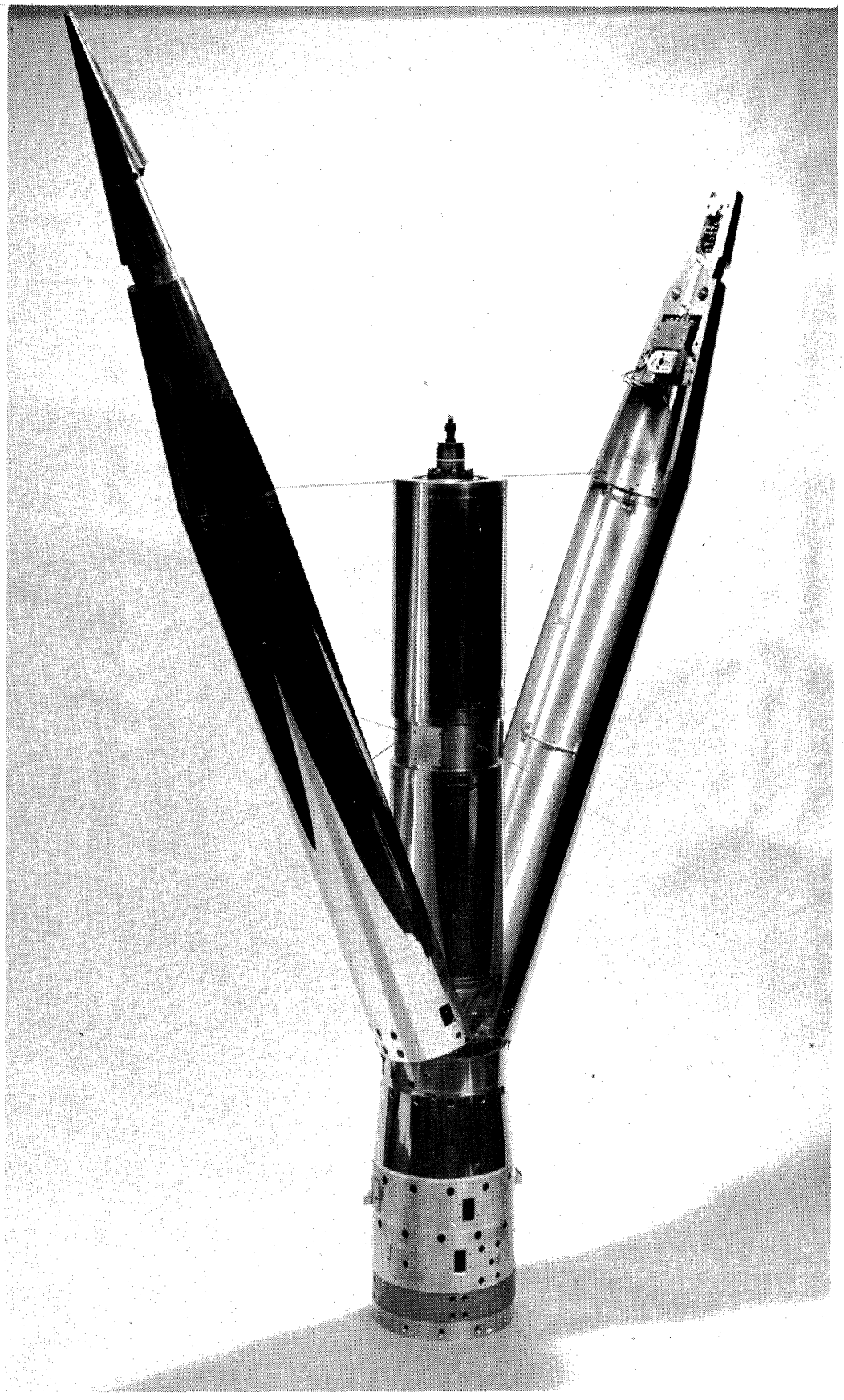

Figure 1. The Thermosphere Probe and nose cone.

QUADRUPOLE ION SOURCE CHARACTERISTICS

The ion source employed in the Quadrupole was orginally developed for application in the Explorer 17 Satellite. It is designed to provide a beam of ions proportional to the neutral gas density and focus them into the Quadrupole analyser. It was intended to provide an ionizing region which most ambient gas particles could reach without collision and consequent surface interaction thus permitting direct interpretation of measurements of highly reactive gases (e.g., atomic oxygen).

Ionizing electrons are obtained by thermal emission from a heated tungsten-rhenium filament (Fig. 2). They are accelerated with a grid, forced by a magnetic field to travel along an arc, and collected at the anode (Fig. 2). Ionization of the atmospheric gas particles occurs throughout this arc, but only those particles which are ionized in the shaded region of the arc are focused into the analyzing section of the instrument.

The focusing of the particles is accomplished with a repeller grid and an internal lens system. The outer screen is kept at zero potential to nullify the effect of the electric fields used in the Quadrupole ion source on the other instruments in the probe and has a negligible effect on the measurement itself. The inner grid is at a potential which simultaneously repels ambient atmospheric ions and forces the ionized gas particles in the direction of the lens system. The ions enter the lens system through an orifice in the accelerator electrode. The lens system establishes a field which focuses the ion beam into the analyser section.

To relate the current of the ion beam to the neutral gas density, it is necessary to establish a relationship between the ambient particle density and the density in the shaded region (Fig. 2). This relationship and the laboratory calibration of the Quadrupole permits the determination of the ambient gas density in terms of the ion current measured by the Quadrupole.

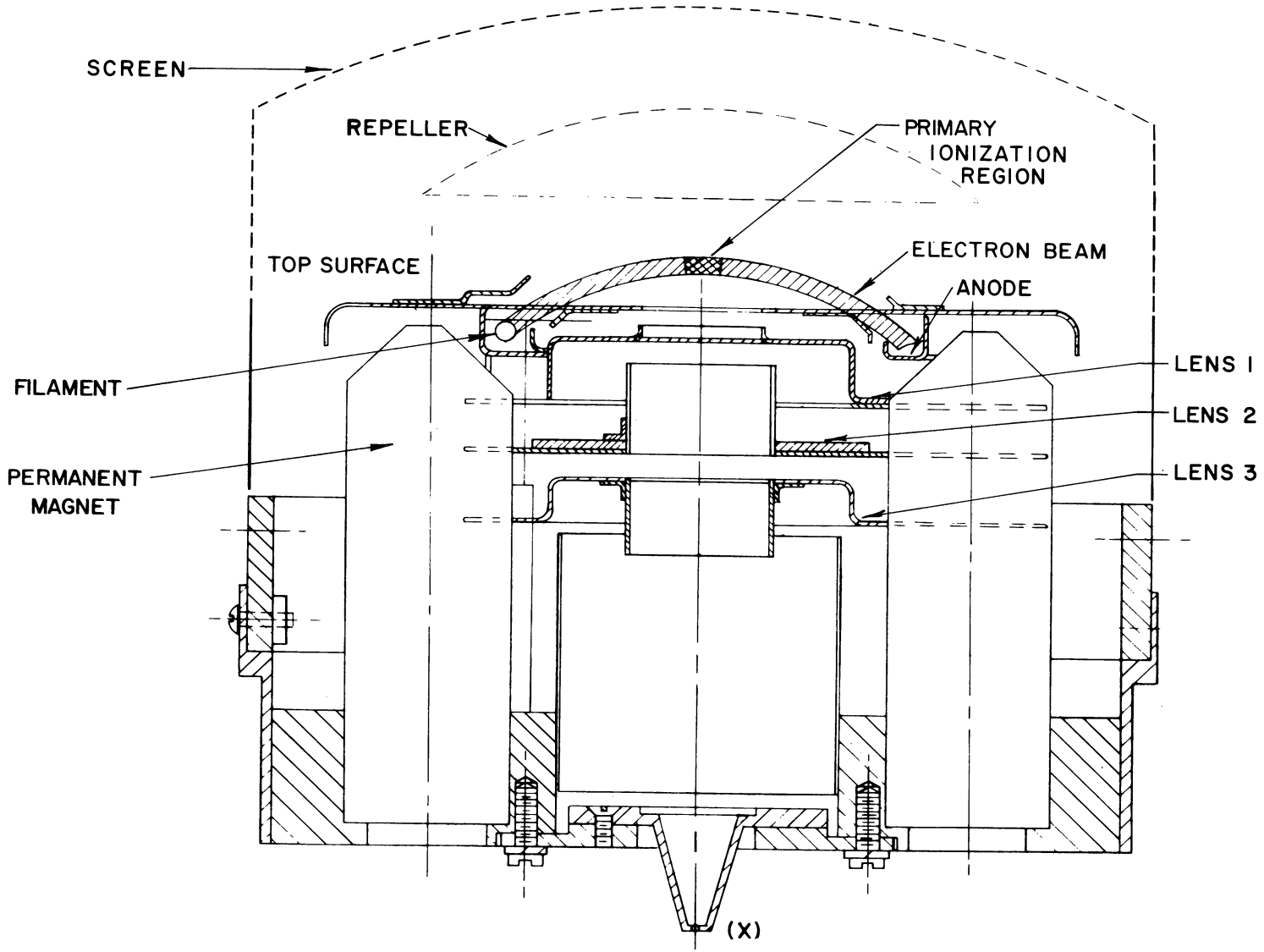

Figure 2. Cross-section of the Quadrupole ion-source and lens chamber with the electron beam trajectory.

DENSITY IN THE IONIZATION REGION

Because of the low ambient gas density in the thermosphere, the mean free path of the particles is much larger than the dimensions of the probe. As a result, viscous effects can be neglected and each particle can be regarded independently of all others.

The density of any one gas in the ionization region can be regarded as the sum of six different contributions:

I. Direct streaming particles; those which enter the ionization region without having interacted with the probe.

II. Particles which strike the top deck;

a. Specularly reflected particles

Those which strike the deck and reverse their velocity normal to the deck.

b. Diffusely reflected particles

Those which strike the deck and bounce off according to the cosine law and keep their original velocity.

c. Diffusely reflected and accommodated particles

Those particles which strike the deck and are re-emitted according to the cosine law but remain on the deck long enough to become accommodated to the temperature of the deck and, therefore, change their characteristic velocity.

III. Particles from the orifice

Those particles which enter through the accelerator orifice without ionization and exit (through the orifice) after accommodating to the ion source temperature.

IV. Particles which emanate from surfaces of the instrument; herein called background.

Particles reflected from the external grids into the ionizing region are estimated to be less than 2% of the total and their contribution to the density in the ionizing region is neglected.

The total density n_t can then be written,

$$n_t = \underset{\text{direct}}{n} + \underset{\text{specular}}{a_1 n} + \underset{\text{diffuse}}{a_2 n} + \underset{\text{diffuse acc.}}{a_3 n} + \underset{\text{orifice}}{n} + \underset{\text{background}}{n}$$

The coefficients a_1, a_2 and a_3 denote the ratios of number of particles leaving the deck in specular, diffusive or thermally accommodated reflection to the total number of particles striking the deck. Regarding the particles reflected from the deck as three distinct groups is an approximation, since in reality particles come off the deck according to a distributuion which is between specular and diffuse and with a temperature between their original one and that of the deck. However, little success has been met with in treating them as such, so this approximation has been made.

CALCULATIONS

I. DIRECT STREAMING

The density due to direct streaming has been calculated assuming that the gas has the Maxwell Boltzmann velocity distribution. If a coordinate system is fixed to the source (see Fig. 3), the number of particles per unit area and unit time in the velocity interval $\vec{v} + d\vec{v}$ and $\vec{v}$ entering the ionization region will be:

$$d\vec{\Gamma} = \kappa \vec{v} f(\vec{v}_1\vec{u}) d^3v \qquad (1)$$

where κ is the transparency of the screen, $\vec{v}$ is the velocity of the particles, and

$f(\vec{v},\vec{u}) = n_o \frac{1}{\pi^{3/2}C_o^3} \exp\left(-\frac{(\vec{v}-\vec{u})^2}{C_o^2}\right)$ is the Maxwell Boltzmann velocity distribution of a moving medium

n_o = ambient particle density

$C_o = \frac{2kT_o}{m}$ most probably thermal velocity

k = 1.38×10^{-23} Joules /°K Boltzmann constant

T_o = absolute gas temperature °K

m = mass of particle

$\vec{u}$ = velocity of the instrument

$S = \frac{|\vec{u}|}{C_o}$ = speed ratio

$S_z = \frac{u_z}{C_o}$ = z component of the speed ratio

From the flux Equation (1), the density is obtained by dividing by the velocity. Referring to Fig. 3, it can be seen that the only particles which reach the ionization region will be those which are not shadowed by the cylinder. Thus, if the velocity distribution is integrated over the velocity space, the cone of half angle θ_1 must be excluded. It is more convenient, however, to integrate over the cone and subtract its contribution from the total density n_o. The number density in the ionizing region resulting from the flow through the cone of half angle θ_1 in cylindrical coordinates is:

$$n_c = n_o \frac{1}{\pi^{3/2}C_o^3} \int_{-\infty}^{0} \int_{0}^{v_z \tan\theta_1} \int_{0}^{2\pi} \exp\left(-\frac{(\vec{v}-\vec{u})^2}{C_o^2}\right) v_r \, d\phi \, dv_r \, dv_z \qquad (2)$$

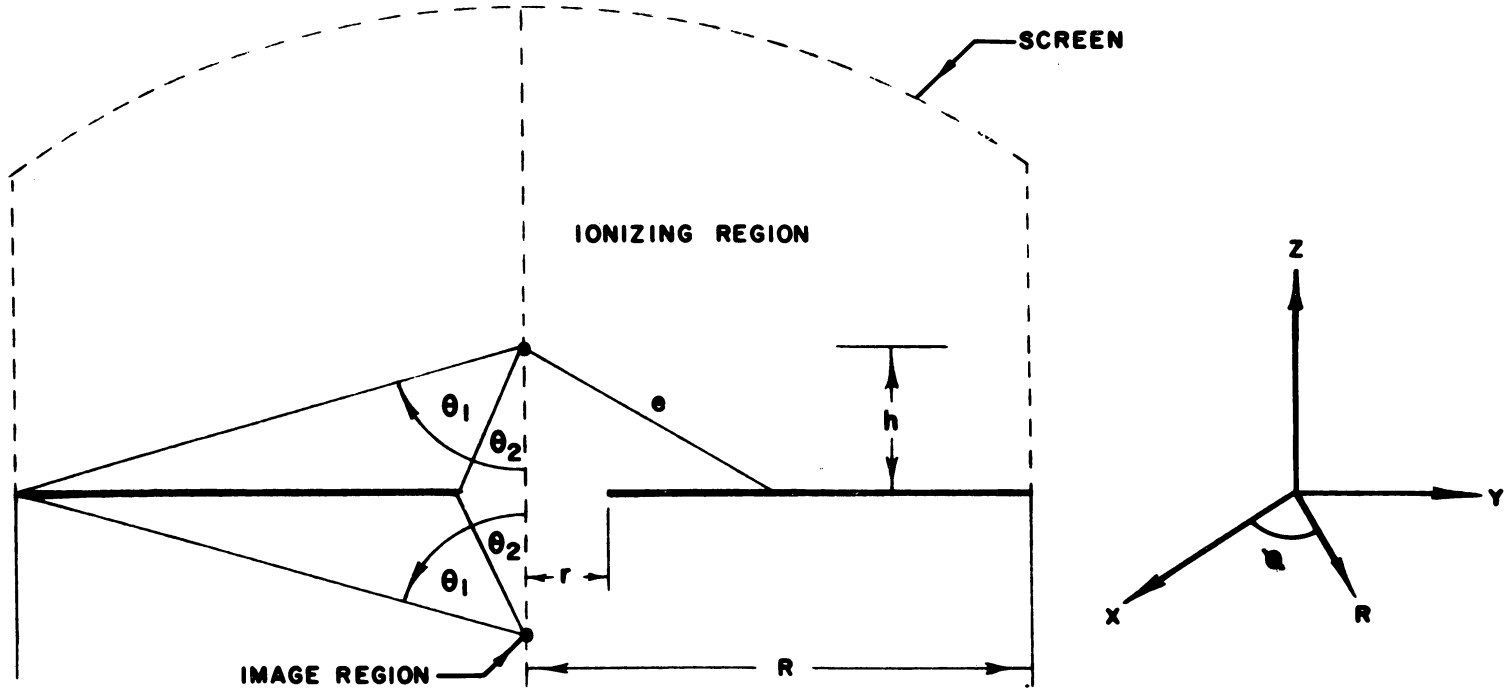

FIG. 3

Figure 3. The simplified model of the geometry of the Quadrupole used for the theoretical development.

With some manipulation (see Appendix) this expression can be reduced to:

$$n_c = \frac{1}{2} n_o \left[1 - \mathrm{erf}(S_z) - \exp\left(-S_z^2\right) M_o - H(S_z, S_r, \theta_1)\right] \tag{3}$$

where

$$H(S_z, S_r, \theta_1) = \exp\left(-(S_z^2 + S_r^2)\right) \sum_{m=1}^{\infty} \frac{S_r^{2m}}{m!} \sum_{k=1}^{m} \sin^{2k}\theta_1 \, M_k \tag{4}$$

$$M_o = \cos\theta_1 \exp\left(S_z^2 \cos^2\theta_1\right)\left[1 - \mathrm{erf}\left(S_z \cos\theta_1\right)\right] \tag{5}$$

$$M_1 = \left(\frac{1}{2} + S_z^2 \cos^2\theta_1\right) M_o - S_z \cos^2\theta_1 \frac{1}{\sqrt{\pi}} \tag{6}$$

$$M_k = \frac{1}{k}\left\{\left[S_z^2 \cos^2\theta_1 + \frac{1}{2}(4k - 3)\right] M_{k-1} - \frac{1}{2}(2k - 3) M_{k-2}\right\} \tag{7}$$

The direct streaming is then given as:

$$n_{\text{direct}} = \kappa(n_o - n_c) =$$

$$\kappa\frac{n_o}{2}\left[1 + \mathrm{erf}(S_z) + \exp\left(-S_z^2\right) M_o(S_z, \theta_1) + H(S_z, S_r, \theta_1)\right] \tag{8}$$

II. REFLECTION FROM THE SURFACE

a. Specularly Reflected Particles

The flow due to specularly reflected particles can be calculated by considering the flow into the image of the source as indicated in Fig. 3. The calculations are identical to those of the previous paragraph except that the difference of the flow through the cones of half angle θ_1, and θ_2 has to be found and S_z has to be replaced by $(-S_z)$.

We have

$$n_{\text{reflect.}} = \kappa\left(n_{c\theta_1} - n_{c\theta_2}\right) \tag{9}$$

where the

$$n_{c\theta} = \frac{1}{2} n_o \left[1 - \mathrm{erf}(S_z) - \exp\left(-S_z^2\right) M_o(-S_z, \theta) - H(-S_z, S_r, \theta)\right] \tag{10}$$

or

$$n_{\text{reflect.}} = \frac{\kappa n_o}{2}\left\{\exp\left(-S_z^2\right)\left[M_o(-S_z,\theta_2) - M_o(-S_z,\theta_1)\right] + H(-S_z,S_r,\theta_2) - H(-S_z,S_r,\theta_1)\right\} \quad (11)$$

and $M_o(\theta)$ and $H(S_z,S_r,\theta)$ are given in Equation (4) to (7).

b. Diffusively Reflected Particles

Here we consider those particles which collide with the top surface but do not thermally accommodate to the surface. Due to the roughness of the surface, they are reflected diffusively (cosine law) without change in velocity.

The flux through the ionizing region is then the outgoing flux times the solid angle subtended by the surface A as seen from the ionizing region.

We have

$$\Gamma_{\text{source}} = \Gamma_{\text{out}} \frac{\Omega_s}{4\pi} \quad (12)$$

Γ_{out} is the outgoing flux referring to Fig. 3

$$\Omega_s = \int_{\text{surface A}} \frac{dA\cos\theta}{e^2} = \int_{\theta_2}^{\theta_1}\int_0^{2\pi} \sin\theta\, d\phi\, d\theta$$

$$= 2\pi(\cos\theta_2 - \cos\theta_1) \quad (13)$$

Equating the incoming and outgoing flux on the surface, we obtain the surface density n_s as a special case of equation (8) ($\theta_1 = 90°$)

$$n_s = \kappa n_o\left[1 + \text{erf}(S_z)\right] \quad (14)$$

and the density in the ionizing region

$$n_{\text{diffuse}} = n_s\frac{\Omega_s}{4\pi} = \kappa\frac{n_o}{2}\left[1+\text{erf}(S_z)\right][\cos\theta_2 - \cos\theta_1] \quad (15)$$

c. Thermally Accommodated Particles

Equating the incoming and outgoing surface flux:

$$\kappa\frac{n_o\,\bar{C}_o}{4} f(S_z) = \frac{n_s\,\bar{C}_i}{4}$$

where n_s is the surface density

$\bar{C}_i$ is the average velocity of the emitted particle

$$f(S_z) = \exp\left(-S_z^2\right) + \sqrt{\pi}\, S_z\, [1 + \mathrm{erf}\,(S_z)]$$

This relation was discussed by Spencer, et. al., Ref. 1. Therefore, we obtain for the density in the ionizing region similar to (b) above:

$$n_{acc.} = n_s \frac{\Omega s}{4\pi} = \kappa \frac{n_o}{2} \sqrt{\frac{T_o}{T_i}}\, f(S_z)\, [\cos\theta_2 - \cos\theta_1] \qquad (16)$$

III. STREAMING FROM THE ORIFICE

Following the procedure in II (c), the density in the ionizing region is given as

$$n_{orifice} = \kappa n_o \sqrt{\frac{T_o}{T_i}}\, f(S_z)\, \frac{\Omega_o}{4\pi} \qquad (17)$$

where Ω_o is the solid angle subtended by the orifice as seen from the ionizing region

It can be written

$$\Omega_o = 2\pi\, (1 - \cos\theta_2) \qquad (18)$$

and the orifice term becomes

$$n_{orifice} = \kappa \frac{n_o}{2} \sqrt{\frac{T_o}{T_i}}\, f(S_z)\, (1 - \cos\theta_2) \qquad (19)$$

Inevitably, surface absorbed gases are carried to the region of measurement. These gases then emanate in flight at a rate assumed constant and contribute to the particle density in the ionizing region. This is the background contribution.

RESULTS

The ratio of the first five terms to the ambient number density computed from the equations above are plotted in Figs. 4-6 as functions of the angle of attack α, where α is defined as the angle between the normal to the top deck and the velocity vector, and $S_z = S \cos \alpha$ and $S_r = S \sin \alpha$. The values S = 1, 2, 3 cover the range seen during a normal Thermosphere Probe flight. The ratio of total density to ambient density is also plotted in Fig. 7 as a function of α for the three values of S.

In this total, no specular reflection term is included ($a_1 = 0$). It has been assumed that on a molecular scale, the surface of the top deck is rough enough to eliminate the possibility of specular reflection.

Since the experimentally measured thermal accommodation coefficients for "almost" clean surfaces are on the order of 0.2, a_3 was taken as 0.2 and a_2 as 0.8. For the Quadrupole source, parameters θ_1 and θ_2 are $\theta_1 = 78.79°$ and $\theta_2 = 37.9°$.

Clearly, the surface terms are major contributors at small angles of attack. Large errors could, therefore, be caused by uncertainties in the coefficients $a_{1,2,3}$. Since the surface terms vary more rapidly with the angle of attack than does the direct streaming term, the particle density in the ionizing region will be less sensitive to the coefficients $a_{1,2,3}$ at large angles of attack. However, at large angles of attack other limitations such as the uncertainty in the aspect information become more significant.

For the measurement of atomic oxygen, the orifice contribution will be reduced since much of the atomic oxygen will recombine in collisions behind the orifice. If the recombination coefficient for atomic oxygen on the material used for the deck and walls of the source is known, the effect of recombination can be calculated. In Fig. 2 a detailed view is given of the chamber behind the orifice of the ion source. The chamber is connected to the ambient atmosphere through the orifice and the annulus formed by the base of the ground screen and the deck. The Quadrupole analyzer, which is separately vented, is connected to the chamber by the small nozzle (x). The gas flow through this nozzle can be neglected. If the number density of oxygen atoms entering the chamber through the orifice and the annulus is known, and the probability that any one particle will leave after one bounce is also known, then the number of particles leaving after any bounce can be calculated. If recombination occurs and γ is the probability of recombining after one bounce, the number of oxygen atoms leaving after one bounce is $\Delta n_1 = n_o p(1-\gamma)$ where n_o is the initial number density of oxygen atoms and p is the probability of leaving after one bounce. After two bounces

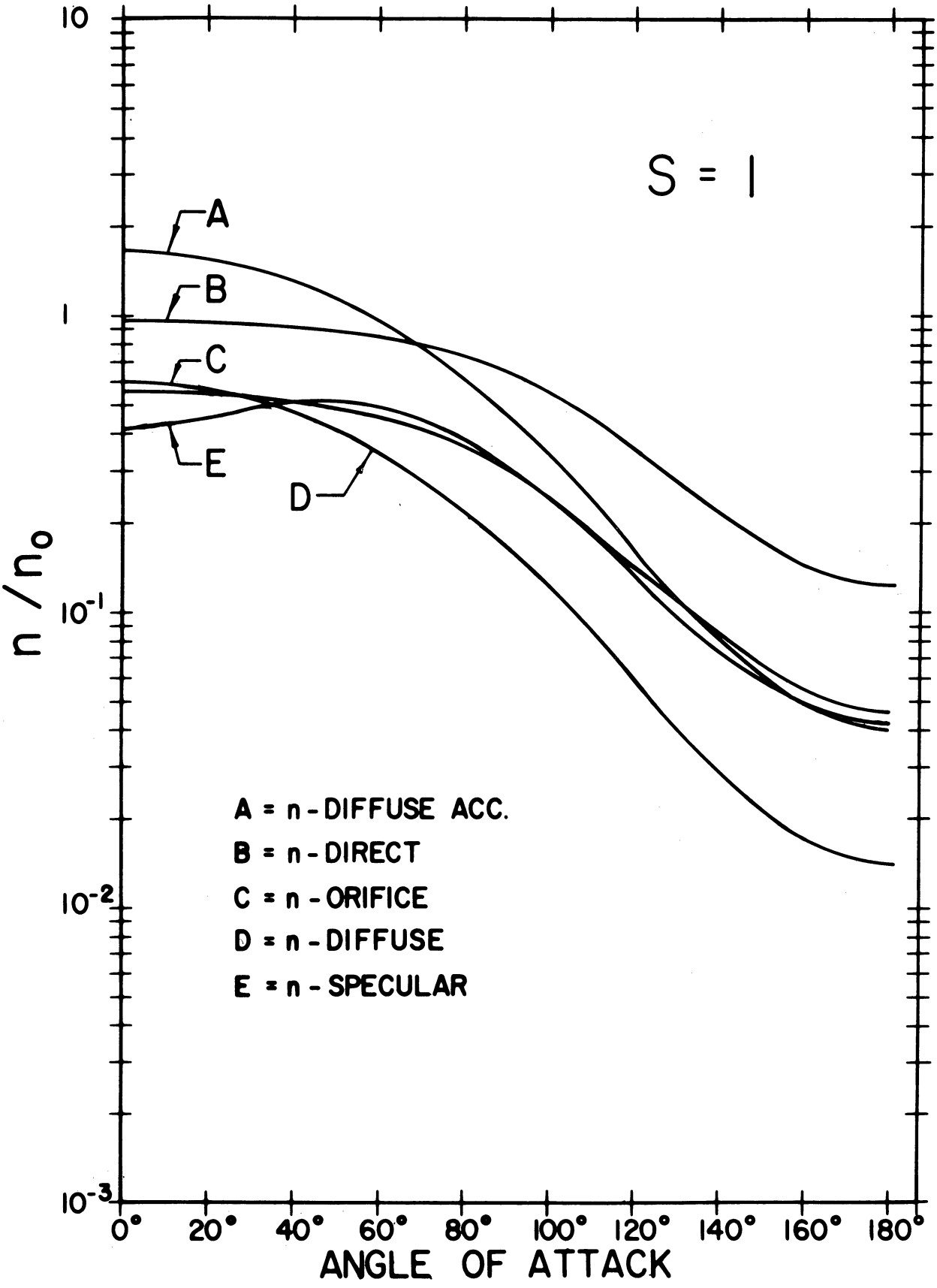

Figure 4. Theoretically derived contributions to the density in the ionizing region versus angle of attack for S = 1.

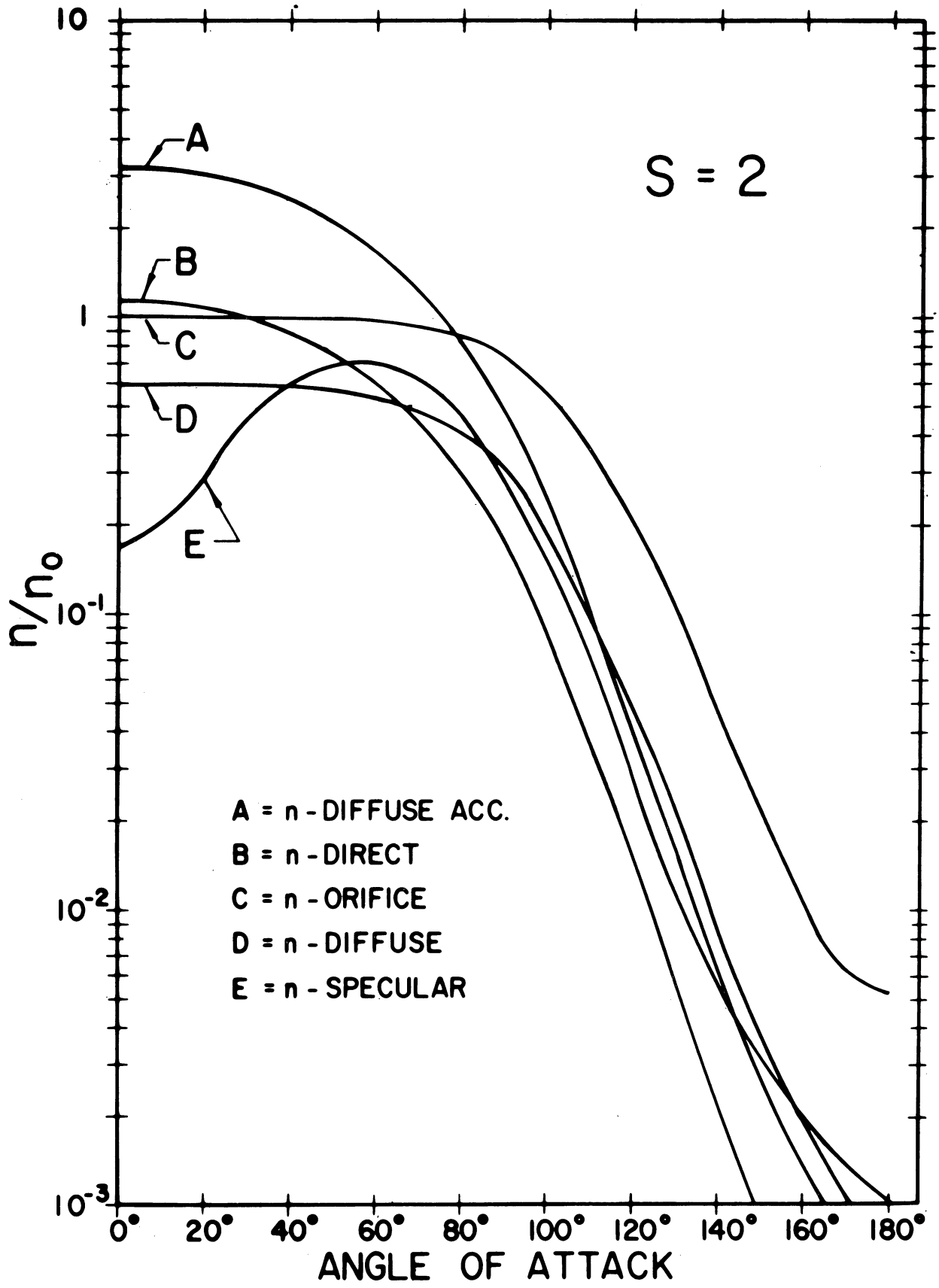

Figure 5. Theoretically derived contributions to the density in the ionizing region versus angle of attack for S = 2.

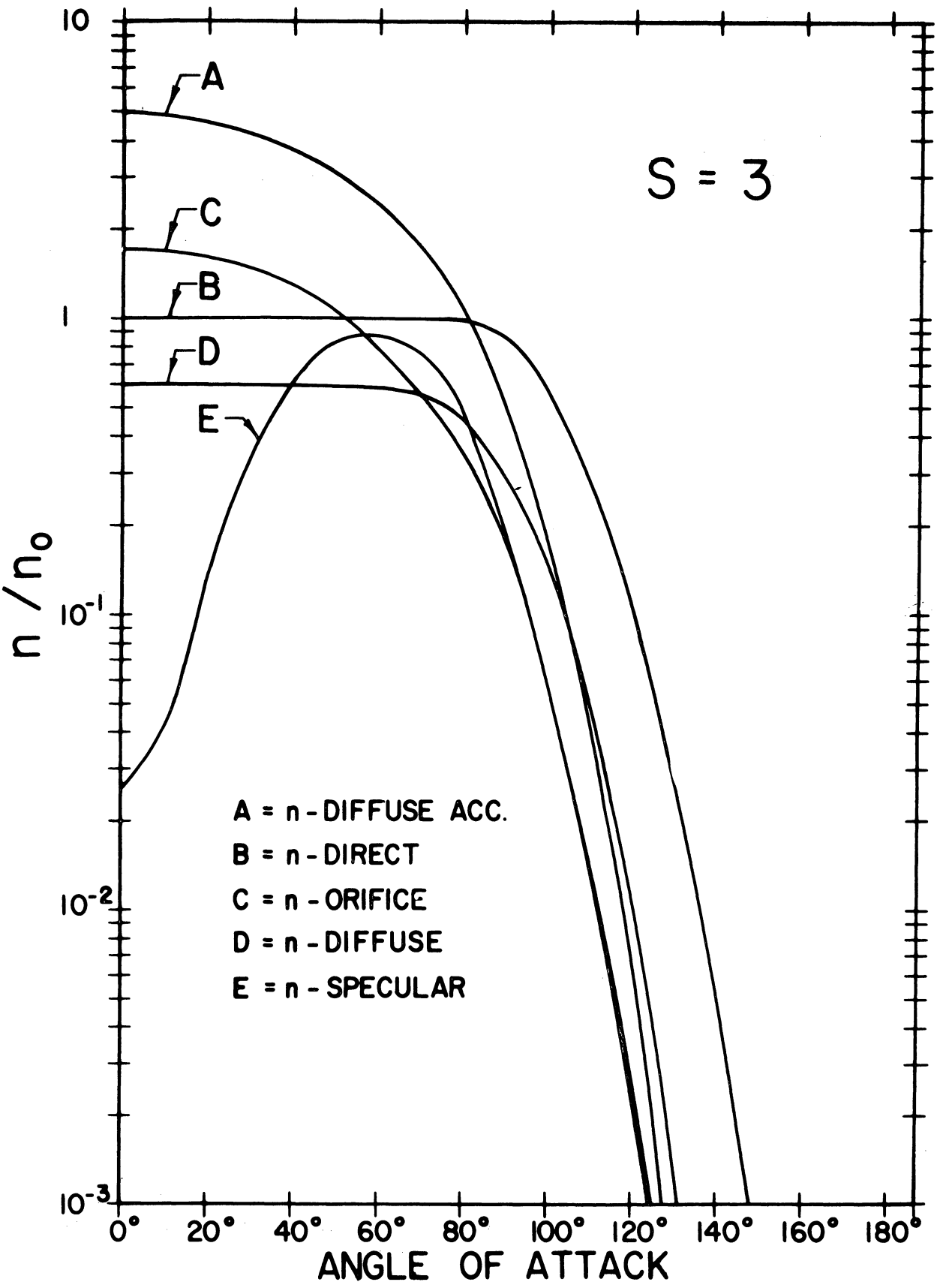

Figure 6. Theoretically derived contributions to the density in the ionizing region versus angle of attack for S = 3.

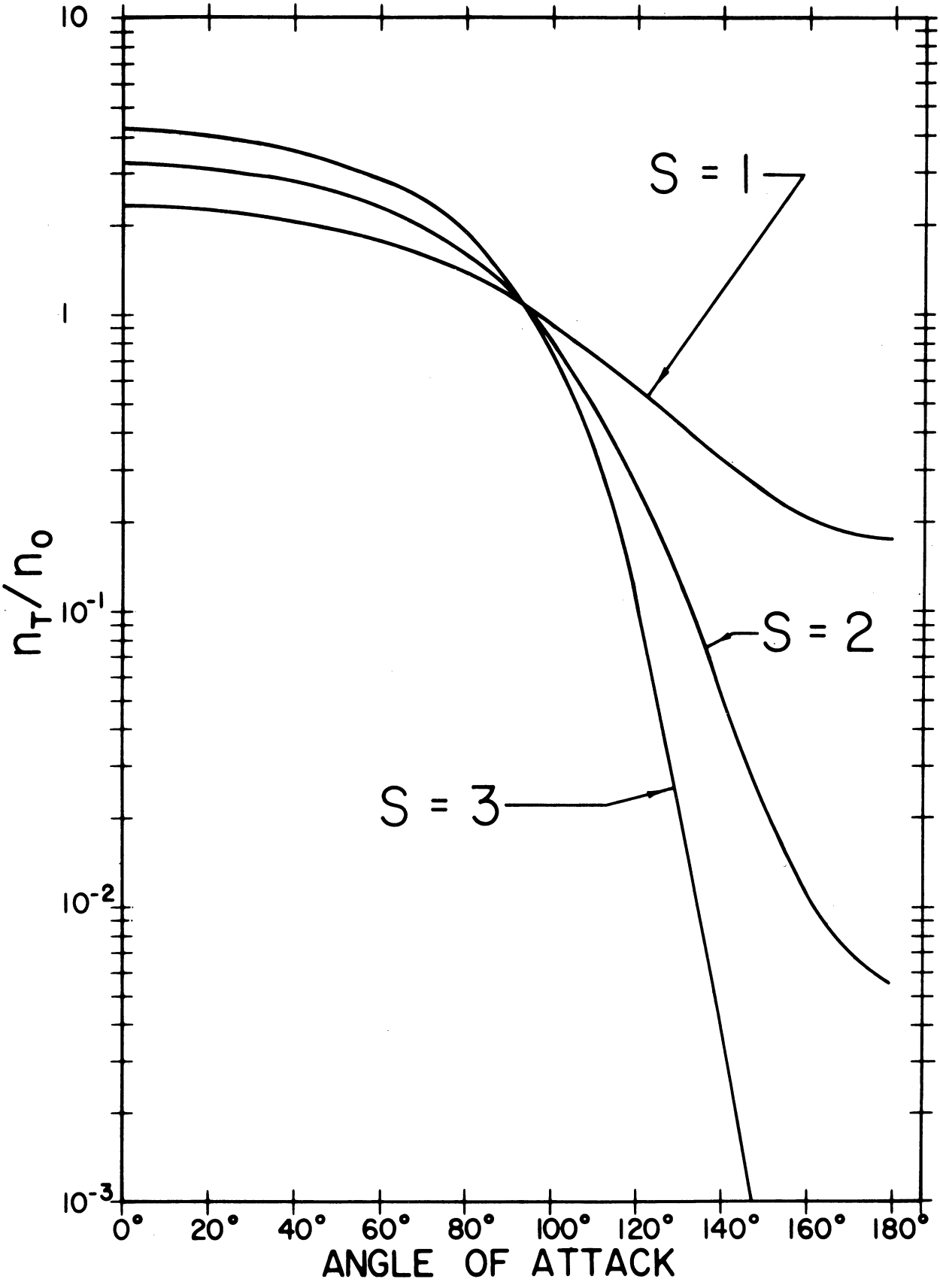

Figure 7. The theoretical density in the ionizing region versus angle of attack with $a_1 = 0$, $a_2 = .8$ and $a_3 = .2$.

$$\Delta n_2 = p(1 - \gamma)\ [n_o\ (1 - \gamma) - \Delta n_1] \tag{20}$$

$$= p\ n_o\ (1 - p)\ (1 - \gamma)^2\ . \tag{21}$$

$$\Delta n_i = pn_o\ (1 - p)^{i - 1}\ (1 - \gamma)^i \tag{22}$$

The total number of oxygen atoms which leave the orifice is then

$$n(o) = pn_o\ (1 - \gamma) + pn_o\ (1 - \gamma)^2\ (1 - p) + \ . \ . \ . \ + pn_o\ (1 - \gamma)^m\ (1 - p)^{m-1} \tag{23}$$

This series terminates due to the fact that a fraction of a particle cannot exist in the gauge. m is, therefore, the first number such that $n_o\ Vp(1 - p)^{m-1}\ (1 - \gamma)^m \leq 1$ where V is the volume of the chamber. Summing the series, which is geometric

$$n(o) = n_o p(1 - \gamma)\ \frac{1 - [(1 - p)\ (1 - \gamma)]^m}{1 - (1 - p)\ (1 - \gamma)} \tag{24}$$

The term $[(1-p)\ (1-\gamma)]^m$ will be negligible, since $[(1-p)\ (1-\gamma)]^m \leq (1/Vn_o)\ [(1-p)/p]$, Vn_o is expected to be at least 10^8 and it will be shown that $p \approx 10^{-2}$. Therefore, $[(1-p)(1-\gamma)]^m \approx 10^{-6}$ and

$$n(o) = n_o\ \frac{p(1 - \gamma)}{1 - (1 - p)\ (1 - \gamma)} = n_o\ \frac{1}{1 + \frac{\gamma}{p(1 - \gamma)}} \equiv n_o R \tag{25}$$

The probability of escape after one bounce can be estimated by considering the time response of the gauge. If at a given time, n_o particles are in the chamber, and these particles alone are considered, then the particle density will decrease exponentially with time $n_{(t)} = n_o e^{-t/\tau}$, where τ is the chamber time constant. τ is the ratio of the volume of the chamber to the gas conductance of the orifice and the annulus. $\tau \approx (V/1/4\ \sigma\bar{v})$, where V is the volume of the chamber, $1/4\ \sigma\ \bar{v}$ is the conductance, σ is the total area of openings, and $\bar{v}$ is the average velocity of the gas particles. If t_o is the average time for a particle to travel from one wall to another, then the decrease in the number of particles after each bounce is given by

$$\Delta n = n_o(t) - n_o(t + t_o) \tag{26}$$

After the i^{th} bounce

$$\begin{aligned}\Delta n_i &= n_o\,[(i-1)t_o] - n_o(it_o)\\ &= n_o\left[\exp\left(-\frac{(i-1)\,t_o}{\tau}\right) - \exp\left(-i\frac{t_o}{\tau}\right)\right]\\ &= n_o\left[1 - \exp\left(-\frac{t_o}{\tau}\right)\right]\exp\left(-(i-1)\frac{t_o}{\tau}\right)\end{aligned} \tag{27}$$

comparing this to equation 22 and disregarding recombination.

$$\Delta n_i = pn_o(1-p)^{i-1} = n_o\left[1 - \exp\left(-\frac{t_o}{\tau}\right)\right]\exp\left(-(i-1)\frac{t_o}{\tau}\right) \tag{28}$$

we obtain $p = 1 - \exp\left(-t_o/\tau\right)$. This reduces to $p \approx t_o/\tau$ if $t_o/\tau \ll 1$. t_o can be approximated by considering a characteristic length of the chamber l, and the average velocity of the gas, to $= l/\bar{v}$. Then $p = (1-\exp(-l\sigma/4V))$. For the Quadrupole, $\sigma \cong .8$ cm^2, $V = 50$ cm^3, $l \cong 3$ cm and $p \cong 1.2 \times 10^{-2}$. With these values, the ratio R of the number of oxygen atoms leaving to those entering has been computed as a function of γ, and the results are plotted in Fig. 8. Since the value of p has been approximated and since the method itself is an approximation, this function has also been plotted for p having the values 10^{-1} and 10^{-3} to estimate possible errors. As can be seen, for most values of γ, a change in p causes a large variation in the value of R. Only when γ is greater than .5 do variations in p have little effect; and in this case, essentially all the atomic oxygen has recombined. Other possibilities which also lead to predictable results include: (1) the use of surfaces that absorb atomic oxygen completely and (2) determination of the time constant of the gauge more exactly by direct experiment.

If p is determined with sufficient accuracy and a material with an established γ can be chosen, then the ratio of the number of atomic oxygen atoms leaving to those entering will be known. In this case, the densities of atomic oxygen and molecular oxygen in the ionization region are

$$n(o) = \underset{\text{direct}}{n(o)} + (1-\gamma)\left[\underset{\text{spec.}}{a_1 n(o)} + \underset{\text{diffuse}}{a_2 n(o)} + \underset{\text{diffuse acc.}}{a_3 n(o)}\right] + \underset{\text{orifice}}{R\,n(o)} \tag{29}$$

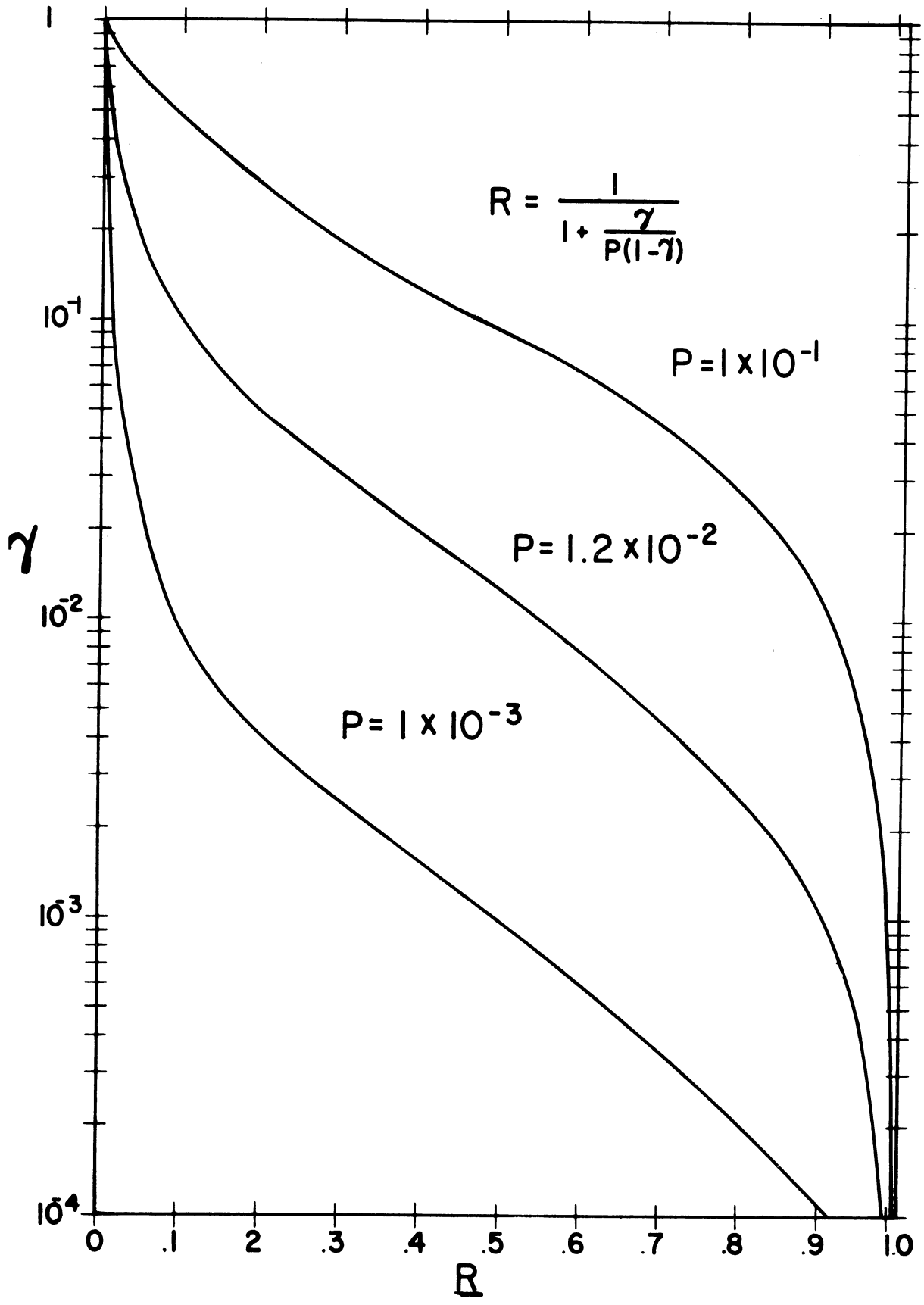

Figure 8. The recombination probability for atomic oxygen versus recombination coefficient of the inner surfaces.

$$n(O_2) = \underset{\text{direct}}{n(O_2)} + \underset{\text{spec.}}{a_1' n(O_2)} + \underset{\text{diffuse}}{a_2' n(O_2)} + \underset{\text{diffuse acc.}}{a_3' n(O_2)} + \underset{\text{orifice}}{n(O_2)}$$

$$+ \frac{\gamma}{2} \left[\underset{\text{spec.}}{a_1'' n(o)} + \underset{\text{diffuse}}{a_2'' n(o)} + \underset{\text{diffuse acc.}}{a_3'' n(o)} \right] + \frac{1}{2} (1 - R) \underset{\text{orifice}}{n(o)} \tag{30}$$

The prime on the a's take into account the possibility of different surface reactions for O, O_2 and recombined O.

DATA REDUCTION

The ambient particle density can be, in principle, obtained from Equation (1) provided all the parameters, including the ambient temperature, are known. It is, however, more convenient to take, as is done in the Omegatron experiment, the difference of two measurements of opposite orientation, Ref. 1.

$$\Delta n_i = n_i(S_z) - n_i(-S_z)$$

$$= \underset{\text{direct}}{n(S_z)} - \underset{\text{direct}}{n(-S_z)} + a_1[\underset{\text{reflect}}{n(S_z)} - \underset{\text{reflect}}{n(-S_z)}] +$$

$$a_2 n_o A \operatorname{erf}(S_z) + a_3 n_o A\sqrt{\frac{T_o}{T_i}}\sqrt{\pi}\, S_z + n_o B\sqrt{\frac{T_o}{T_i}}\sqrt{\pi}\, S_z \qquad (31)$$

where A and B are constants depending on the source geometry only (see Fig. 3)

$$A = \cos\theta_2 - \cos\theta_1 = \frac{1}{1+(\frac{r}{h})^2} - \frac{1}{1+(\frac{R}{h})^2} \qquad (32)$$

$$B = 1 - \cos\theta_2 = 1 - \frac{1}{1+(\frac{r}{h})^2} \qquad (33)$$

and if we assume no specular reflection

$$\Delta n_i = \underset{\text{direct}}{n(S_z)} - \underset{\text{direct}}{n(-S_z)} + n_o[a_2 A \operatorname{erf}(S_z) + (a_3 A + B) \qquad (34)$$

$\sqrt{\frac{T_o}{T_i}}\sqrt{\pi}\, S_z]$; if $S_{i_z} \equiv \sqrt{\frac{T_o}{T_i}}\, S_z = \frac{u_z}{C_i}$ equation (34) becomes

$$\Delta n_i = \underset{\text{direct}}{n(S_z)} - \underset{\text{direct}}{n(-S_z)} + no[a_2 A \operatorname{erf}(S_z) + (a_3 A + B)\sqrt{\pi}\, S_{i_z}] \qquad (35)$$

The first three terms in (35) contain the ambient temperature, but this can be obtained independently from the Omegatron measurement, or from an iteration process by solving for n_o at different S_z values. For large values of S and S_z, these terms are insensitive to small variations in S and S_z. If $S > 1.5$ and $S_z > 2/3\ S$ we get

$$n_i \cong n_o \left[1 + a_2 A + (a_3 A + B)\sqrt{\pi}\, S_{i_z}\right] \tag{36}$$

The expressions for atomic oxygen are

$$\Delta n_i(O) = \underset{\text{direct}}{n(O)(S_z)} - \underset{\text{direct}}{n(O)(-S_z)} + n_o(O)$$

$$\left\{a_2 (1-\gamma)\, A\, \text{erf}\,[S_z(O)] + [a_3(1-\gamma)\, A + RB]\sqrt{\pi}\, S_{i_z}(O)\right\} \tag{37}$$

and if we assume that the recombined oxygen fully accommodates to the surface temperature, we have for molecular oxygen

$$\Delta n_i(O_2) = \underset{\text{direct}}{n(O_2)\,(S_z)} - \underset{\text{direct}}{n(O_2)(-S_z)} +$$

$$n_o(O_2)\left\{a_2' A\, \text{erf}\,[S_z(O_2)] + (a_3' A + B)\sqrt{\pi}\, S_{i_z}(O_2)\right\} +$$

$$\frac{n_o(O)}{\sqrt{2}}\,[\gamma A + (1-R)B]\sqrt{\pi}\, S_{i_z}(O) \tag{38}$$

for large S and S_z and realizing that $S_{i_z}(O) = \frac{1}{\sqrt{2}} S_{i_z}(O_2)$

$$\Delta n_i(O) = n_o(O)\left\{1 + a_2 A(1-\gamma) + [a_3 A(1-\gamma) + RB]\sqrt{\pi}\, S_{i_z}(O)\right\} \tag{39}$$

$$\Delta n_i(O_2) = n_o(O_2)\,[1 + a_2' A + (a_3' A + B)\sqrt{\pi}\, S_{i_z}(O_2)] +$$

$$\frac{n_o(O)}{2}\,[\gamma A + (1-R)\,B]\sqrt{\pi}\, S_{i_z}(O_2) \tag{40}$$

The data can also be reduced in another way. As can be seen from the graphs of n/n_o, there is an angle just greater than $\alpha = 90°$ at which the density is approximately independent of S. This can also be demonstrated analytically by expanding n/n_o in a Taylor Series in α around the angle $\alpha = 90°$. The first derivative of the first term of n_i/n_o with respect to α can be summed, and the

first derivatives of the remaining terms are easily found. To first order in $\Delta\alpha$, n/n_o is

$$\frac{n_i(S,\alpha)}{n_o} = \frac{n_i(S,\pi/2)}{n_o} + \frac{\partial}{\partial\alpha}\left(\frac{n_i(S,\alpha)}{n_o}\right)\Big|_{\alpha = \pi/2}\Delta\alpha \qquad (41)$$

$$\frac{n_i(S,\alpha)}{n_o} = \frac{1}{2}\left[1 + \cos\theta_1 + H(0, S_r, \theta_1) + a_2A + a_3A\sqrt{\frac{T_o}{T_i}} + B\sqrt{\frac{T_o}{T_i}}\right] -$$

$$\left[\frac{1}{\sqrt{\pi}}a_2A + \frac{\sqrt{\pi}}{2}\sqrt{\frac{T_o}{T_i}}\,(a_3A + B) +\right.$$

$$\left.\frac{1}{\sqrt{\pi}}\sin^2\theta_1 \exp\left(-S^2\cos^2\theta_1\right)\right] S\Delta\alpha$$

Solving the equality $n(S_1,\alpha)/n_o = n(S_2,\alpha)/n_o$ for pairs of (S_1,S_2) where $0 < S_1 \leq 3.5$ and $0 < S_2 \leq 3.5$, it is found that $.8° \leq \Delta\alpha \leq 4°$. Therefore, the density ratio in the range of α between 91.8° and 94° is essentially independent of S. This constant value is dependent on temperature, but in the temperature range of T = 500°K to 1000°K the constant changes by only 15%. Since the temperature can be determined from the Omegatron Experiment, the constant can be calculated and the ambient density may be read at an angle between α = 90.8° and α = 94° with relatively little error. The error resulting from the uncertainty of a_2 and a_3 is of second order since their sum must be unity thus compensating first order effects. Background contribution can be found by taking readings at angles of attack near 180° where the ambient particles contribute very little to the source density.

CONCLUSION

The atmospheric density and composition can be determined from measurements of the Thermosphere Probe Quadrupole experiment by using the relationships derived herein. Even in this relatively open ion source, particles which undergo collisions with the instrument contribute significantly to the measured current and must be rigorously taken into account. Atomic oxygen and other reactive gases are subject to recombination and other chemical changes on collision with surfaces and all gases are subject to thermal transformations. The principal limitations in the accuracy of the measurements made by this open source instrument are expected to result from uncertainties in the accommodation and recombination coefficients involved in the gas surface interactions. These uncertainties can be minimized by careful choice of materials and by maintaining high standards of surface cleanliness.

A Quadrupole-Omegatron combination will be flown on a Thermosphere Probe in August 1966. The simultaneous measurement by the Omegatron of atmospheric nitrogen will provide an independent determination of the same parameters of the earth's atmosphere for meaningful comparison thus permitting testing the validity of the derived relationship and the assumptions involved.

APPENDIX

An evaluation of the integral in velocity space of the Maxwell-Boltzmann distribution function over a cone of half-angle Θ_1 with its axis on the z axis. (Ref.2)

$$n_c = \frac{n_o}{\pi^{3/2} C_o^3} \int_{-\infty}^{o} \int_{o}^{v_z \tan\Theta_1} \int_{o}^{2\pi} \exp - \left(\frac{\vec{v}-\vec{u}}{C_o}\right)^2 v_r \, d\varphi \, dv_r \, dv_z \qquad (A.1)$$

$$= \frac{n_o}{\pi^{3/2} C_o^3} \int_{-\infty}^{o} \exp - \frac{(v_z-u_z)^2}{C_o^2} \int_{o}^{v_z \tan\Theta_1} v_r \exp - \left(\frac{v_r^2+u_r^2}{C_o^2}\right) \int_{o}^{2\pi} \exp - \left(- \frac{2 v_r u_r \cos\varphi}{C_o^2}\right) d\varphi \, dv_r \, dv_z \qquad (A.2)$$

$$\int_{o}^{2\pi} \exp - \frac{2 v_r u_r \cos\varphi}{C_o^2} \, d\varphi = 2\pi \, I_o \left(2 \frac{u_r v_r}{C_o^2}\right) \qquad (A.3)$$

where

$$I_o(x) = \sum_{m=o}^{\infty} \left(\frac{x}{2}\right)^{2m} \frac{1}{(m!)^2} \qquad (A.4)$$

is the hyperbolic Bessel function of zero order.

Equation (A.2) can be written in the form

$$n_c = n_o \frac{2\pi}{\pi^{3/2} C_o^3} \exp - \frac{u_r^2}{C_o^2} \int_{-\infty}^{o} \exp - \frac{(v_z-u_z)^2}{C_o^2} I(v_r, u_r, u_z) dv_z \qquad (A.5)$$

$$I(v_z, u_r, u_z) = \sum_{m=o}^{\infty} \left(\frac{u_r}{C_o}\right)^{2m} \frac{1}{(m!)^2} C_o^2 \int_{o}^{\frac{v_z}{C_o} \tan\Theta_1} y^{2m+1} \exp(-y^2) dy \qquad (A.6)$$

Integrating this we have

$$I(v_z,u_r,u_z) = \frac{1}{2} \sum_{m=0}^{\infty} \left(\frac{u_r}{C_o}\right)^{2m} \frac{C_o^2}{m!} \left\{ 1-\exp \left[\frac{v_z^2 \tan^2 \theta_1}{C_o^2}\right] \sum_{k=0}^{m} \frac{\left(\frac{v_z}{C_o}\right)^{2k} (\tan\theta_1)^{2k}}{k!} \right\} \tag{A.7}$$

Introducing the normalized velocities

$$S_z = \frac{u_z}{C_o} \; ; \quad W = \frac{v_z}{C_o}$$

we have

$$I(W, S_r, S_z) = \frac{1}{2} \sum_{m=0}^{\infty} S_r^{2m} \frac{C_o^2}{m!} \left[1-\exp \left[-(W\tan\theta_1)^2\right] \sum_{k=0}^{m} \frac{(W \tan \theta_1)^{2k}}{k!} \right]$$

$$= \frac{1}{2} C_o^2 \left[\exp \left[-S_r^2\right] - \sum_{m=0}^{\infty} \frac{S_r^{2m}}{m!} \exp \left[-(W\tan\theta_1)^2\right] \sum_{k=0}^{m} \frac{(W \tan \theta_1)^{2k}}{k!} \right] \tag{A.8}$$

and

$$n_c = \frac{1}{2} n_o \left[1 - \operatorname{erf} (S_z)\right] -$$

$$\frac{n_o}{\sqrt{\pi}} \exp \left[-(S_r^2+S_z^2)\right] \sum_{m=0}^{\infty} \frac{S_r^{2m}}{m!} \int_{-\infty}^{0} \exp \left[-(W\tan\theta_1)^2\right] \sum_{k=0}^{m} \frac{(w\tan\theta_1)^{2k}}{k!} \exp \left[-W^2+2S_zW\right] dW$$

$$= \frac{1}{2} n_o \left[1 - \operatorname{erf} (S_z)\right] -$$

$$\frac{n_o}{\sqrt{\pi}} \exp \left[-(S_r^2+S_z^2)\right] \sum_{m=0}^{\infty} \frac{S_r^{2m}}{m!} \sum_{k=0}^{m} \frac{(\tan\theta_1)^{2k}}{k!} \int_{-\infty}^{0} W^{2k} \exp \left[2S_zW-W^2\sec^2\theta_1\right] dW \tag{A.9}$$

$$= \frac{1}{2} n_o \left[1 - \operatorname{erf}(S_z)\right] -$$

$$\frac{n_o}{\sqrt{\pi}} \exp \left[-(S_r^2+S_z^2)\right] \sum_{m=0}^{\infty} \frac{S_r^{2m}}{m!} \sum_{k=0}^{m} \frac{(\tan\theta_1)^{2k}}{k!} J_{k-\frac{1}{2}} (S_z,\theta_1)$$

with

$$J_k\,(S_z,\theta_1) = \int_0^\infty \lambda^{2k+1} \exp\left[-2S_z\lambda - \lambda^2\sec^2\theta_1\right] d\lambda \qquad (A.10)$$

The J_k's have the recursion relation

$$J_k = \frac{1}{2}\cos^2\theta_1\,[\delta_{o,k} + 2kJ_{k-1} - 2S_zJ_{k-\frac{1}{2}}] \qquad (A.11)$$

Separating the m=0 term in order to isolate the dependency of n_c on S_r and defining the quantities M_k given by

$$M_k = (2\sec\theta_1)^{2k}\,J_{k-\frac{1}{2}}\frac{1}{\sqrt{\pi}\,k!} \qquad (A.12)$$

we have

$$n_c = \frac{1}{2}\,n_o\,[1 - \mathrm{erf}(S_z) - \exp\left[-S_z^2\right]M_o - H(S_z,S_r,\theta_1)\,] \qquad (A.13)$$

$$H(S_z,S_r,\theta_1) = \exp\left[-(S_z^2 + S_r^2)\right]\sum_{m=1}^{\infty}\frac{S_r^{2m}}{m!}\sum_{k=1}^{m}\sin^{2k}\theta_1\,M_k \qquad (A.14)$$

$$M_o = \cos\theta_1\exp\left[S_z^2\cos^2\theta_1\right][1 - \mathrm{erf}(S_z\cos\theta_1)\,] \qquad (A.15)$$

$$M_1\,(\tfrac{1}{2} + S_z^2\cos^2\theta_1)\,M_o - S_z\cos^2\theta_1\frac{1}{\sqrt{\pi}} \qquad (A.16)$$

$$M_k = \frac{1}{k}\,\{[S_z^2\cos^2\theta_1 + \frac{1}{2}\,(4k-3)\,]\,M_{k-1} - \frac{1}{2}\,(2k-3)\,M_{k-2}\} \qquad (A.17)$$

REFERENCES

1. Spencer, N. W., Brace, L. H., Carignan, G. R., Taeusch, D. R., and Niemann, H. B., Electron and molecular nitrogen temperature and density in the thermosphere, J. Geophysical Research, 70, 2665-2698, 1965.

2. Hedin, A. E., Avery, C. P., and Tschetter, C. D., An analysis of spin modulation effects on data obtained with a rocket-bourne mass spectrometer, J. Geophysical Research, 69, 4637-4648, 1964.